Use of the Resonance Raman Intensities To Check the Density Functional Theory Derived Force Field of the Free Base Porphine

Mouhsine Tazi, Philippe Lagant, and Gérard Vergoten*,†

CRESIMM, Université des Sciences et Technologies de Lille, UFR de Chimie, Bât C8, 59655 Villeneuve d'Ascq, France

Received: July 20, 1999; In Final Form: October 18, 1999

The vibrational normal modes of the free base porphine (FBP) have been investigated within the framework of the density functional theory (DFT). The scaling of the internal force constants has been performed using a least-squares method, and a general valence force field was deduced for the free base porphine with D_{2h} symmetry. To check the vibrational assignments for the normal modes having the A_g symmetry, the resonance Raman intensities have been predicted. It is shown that the *A* term part of the scattering tensor is able to explain most of the observed resonance Raman enhancements for the electronic transitions lying in the Q band.

Introduction

The free base porphine (FBP) is the starting point for vibrational studies on metalloporphyrins which constitute a template for very important biological functions such as photosynthesis, oxygen transport, and oxidation/reduction mechanisms. A resonance structure with D_{2h} symmetry has been shown to stand for the free base porphyrin leading to an electronic delocalized structure for the ground state.

The resonance Raman, visible absorption, fluorescence, and phosphorescence spectra have been largely investigated,[1,3] and more recently polarized infrared spectra[4] and Raman[5] investigations have been performed on the basis of a force field derived from scaled quantum mechanical studies (SQM).

In the present calculations, we used as in previous studies[6,8] the density functional theory (DFT) approach which takes into account the exchange-correlation corrections needed to correctly reproduce the delocalization effects.

The potential energy distribution (PED) may strongly vary from one specific force field determinated from scaled quantum mechanical studies to another one. To overcome this problem, vibrational studies using isotopomers have been used with success to correctly approach the nature of the normal modes associated with the scaled quantum mechanical force field.

In the present study, we used an additional approach which consists of the prediction of the resonance Raman intensities (RRI) of the vibrational modes belonging to the totally symmetric species. This method permits verification of the potential energy distributions of the A_g normal modes and was applied previously in our group to study nucleic acids[9,12] and aromatic amino acids. It will be shown below that such a method is quite easy to use when regarding the difficulty to predict correct infrared or Raman intensities and, consequently, appears as a complementary tool to obtain a correct force field. Unfortunately the infrared vibrational intensities are not available with the DFT procedure in the Jaguar software.

Materials and Methods

The DFT calculations were performed using the Jaguar software (version 3.0).[13] The B3-LYP exchange functional (Becke-3/parameter/HF/Slater/Becke88/VWN and LYP) was used in addition to the 6-31G(df,p)(5d,7f) basis set.

A calculation at the same level of theory was performed previously by Kozlowski et al.[4,5] The geometry optimization was first done using the Merck force field included in the Spartan program (version 5.0.2)[14] under a constrained D_{2h} geometry. This structure was thereafter treated by the DFT method using a total number of 429 basis functions. No constraints were imposed, and the final geometry remains of the D_{2h} type.

The matrix of second derivatives of the potential energy with respect to the Cartesian coordinates (Hessian matrix) resulting from the DFT optimization was treated using the Redong program of Allouche and Pourcin.[15] The method under consideration consists of the determination (by least-squares methods) of the scaling factors corresponding to the internal or symmetry coordinates leading to the best fit of the theoretical to the experimental vibrational wavenumbers. The force constants can then be expressed in terms of internal or symmetry coordinates if removal of local and/or cyclic redundancies is required.

The free base porphine has 38 atoms and 108 ($3N - 6$) internal degrees of freedom. Under a D_{2h} symmetry, with the *x* and *y* axes lying in the molecular plane the irreducible representation of the fundamental vibrational modes is given by $19A_g + 18B_{1g} + 9B_{2g} + 8B_{3g} + 10B_{1u} + 8A_u + 10B_{1u} + 18B_{2u} + 18B_{3u}$ species, where the A_g, B_{1g}, B_{3u}, and B_{2u} species are related to the in-plane modes.

Figure 1 displays the structure under D_{2h} symmetry, and Table 1 gives the Cartesian coordinates of the optimized geometry. The molecular electrostatic potential (ESP) was fitted to a set of point charges located at the atomic centers. The fit was constrained to reproduce the dipole moment exactly. A total of 160 internal coordinates were used to define the molecule. No symmetry coordinates were defined to remove the redundancies occurring in the pyrrole rings or in the superring for the following reasons: (i) For each pyrrole ring, it is possible to use local symmetry coordinates, but the external substituents ($C_\beta H$ and NH) have to be included for redundancy relations. (ii) The total symmetry coordinates including the external C_mH atoms must be linear combinations of these local symmetry

† E-mail: gerard.vergoten@univ-lille1.fr.

10.1021/jp992490r CCC: $19.00
Published on Web 12/31/1999

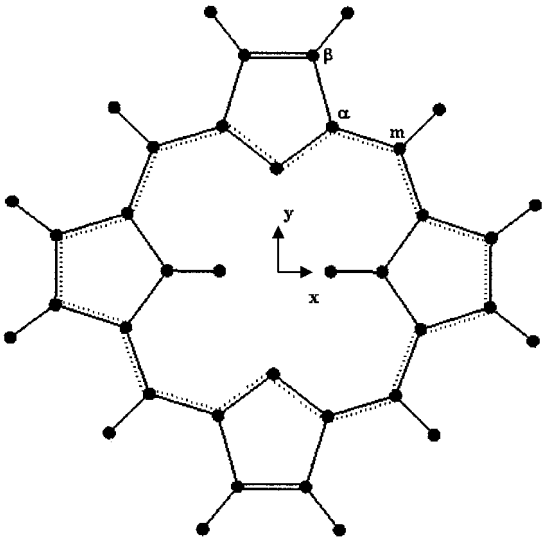

Figure 1. Free base porphine structure under D_{2h} symmetry (taken in the *xy* plane).

TABLE 1: Optimized DFT Cartesian Coordinates for FBP Atoms As Calculated under the D_{2h} Symmetry (*xy* plane) and Their Corresponding Charges (Atomic Units)

atom	atomic no.	*x*	*y*	*Z*	atomic charge
1	7	0.000 00	−2.036 836	0.000 00	−0.450 23
2	1	1.352 02	5.112 69	0.000 00	0.160 50
3	7	0.000 00	2.036 83	0.000 00	−0.450 23
4	1	−1.098 517	0.000 00	0.000 00	0.180 41
5	1	1.098 51	0.000 00	0.000 00	0.180 41
6	7	−2.113 52	0.000 00	0.000 00	−0.189 47
7	7	2.113 52	0.000 00	0.000 00	−0.189 47
8	6	2.893 23	1.131 02	0.000 00	0.282 78
9	6	2.893 23	−1.131 022	0.000 00	0.282 78
10	6	1.085 96	−2.861 657	0.000 00	0.386 24
11	6	−1.085 967	−2.861 657	0.000 00	0.386 24
12	6	−2.893 237	−1.131 022	0.000 00	0.282 78
13	6	−2.893 237	1.131 022	0.000 00	0.282 78
14	6	−1.085 965	2.861 657	0.000 00	0.386 24
15	6	1.085 96	2.861 657	0.000 00	0.386 24
16	1	3.182 83	3.219 54	0.000 00	0.163 88
17	6	0.678 63	4.265 08	0.000 00	−0.269 12
18	6	2.422 87	2.443 95	0.000 00	−0.416 53
19	6	4.258 33	0.686 41	0.000 00	−0.250 23
20	6	2.422 87	−2.443 952	0.000 00	−0.416 53
21	6	−0.678 632	4.265 08	0.000 00	−0.269 12
22	6	−2.422 877	2.443 95	0.000 00	−0.416 53
23	6	−4.258 333	0.686 410 73	0.000 00	−0.250 23
24	6	0.678 63	−4.265 086	0.000 00	−0.269 12
25	1	−3.182 839	3.219 541	0.000 00	0.163 88
26	6	−2.422 877	−2.443 951	0.000 00	−0.416 53
27	6	−4.258 333	−0.686 410	0.000 00	−0.250 23
28	6	4.258 33	−0.686 410	0.000 00	−0.250 23
29	6	−0.678 632	−4.265 086	0.000 00	−0.269 12
30	1	3.182 84	−3.219 541	0.000 00	0.163 88
31	1	−3.182 839	−3.219 541	0.000 00	0.163 88
32	1	1.352 02	−5.112 691	0.000 00	0.160 50
33	1	5.113 85	−1.347 760	0.000 00	0.172 11
34	1	−5.113 856	1.347 760	0.000 00	0.172 11
35	1	5.113 85	1.347 760	0.000 00	0.172 11
36	1	−1.352 022	−5.112 691	0.000 00	0.160 50
37	1	−1.352 022	5.112 691	0.000 00	0.160 50
38	1	−5.113 856	−1.347 760	0.000 00	0.172 11
dipole moment (Debye)		0.000	0.000	0.000	0.000

coordinates to respect the D_{2h} molecular symmetry. (iii) The derived symmetry force constants are typical of the D_{2h} symmetry and cannot be used for the molecule with a different symmetry. (iv) A transformation from the space of nonredundant symmetry coordinates (108) to the space of internal coordinates (160) would reintroduce ring redundancies. As the aim of this work was to select a possible set of internal force constants and transferable scaling factors, no further attempt was done to treat the problem in this way. Comparable assignments in the potential energy distribution can be made between the present work and those obtained from Koslowski et al.[4,5]

TABLE 2: Comparison between Optimized Geometrical Parameters (Å, deg) As Obtained from Different ab Initio Calculations

	DFT/B3LYP (this work)	LDFT[16]	SCF/TZP[17]	MP2/DZP2[18]	exptl[1]
N−H	1.015	1.038	0.99	0.99	
N−C_α	1.37	1.365	1.35	1.36	1.367
(N−C_α)[a]	1.363	1.363	1.34	1.35	1.364
C_β−C_α	1.436	1.423	1.43	1.43	1.438
(C_β−C_α)[a]	1.462	1.445	1.45	1.46	1.463
C_β−C_β	1.372	1.371	1.35	1.35	1.373
(C_β−C_β)[a]	1.356	1.358	1.34	1.34	1.354
C_m−C_α	1.394	1.384	1.38	1.37	1.392
(C_m−C_α)[a]	1.4	1.390	1.39	1.38	1.393
C_β−H	1.080	1.094	1.07	1.06	
(C_β−H)[a]	1.082	1.095	1.07	1.06	
C_m−H	1.086	1.098	1.07	1.07	
H−N−C_α	124.6	125.0	124.4	124.4	
C_α−N−C_α	110.8	110.1	111.1	110.8	109.6
(C_α−N−C_α)[a]	105.5	104.9	106.4	105.1	105.7
N−C_α−C_β	106.5	107.2	106.5	106.9	107.8
(N−C_α−C_β)[a]	111.0	111.4	110.7	111.5	110.9
C_α−C_β−C_β	108.0	107.7	107.9	107.7	107.4
(C_α−C_β−C_β)[a]	106.2	106.9	108.1	105.9	106.3
N−C_α−C_m	125.6	125.6	126.2	125.5	124.8
(N−C_α−C_m)[a]	125.4	125.6	125.9	125.6	125.1
C_α−C_m−C_α	127.1	126.3	126.6	126.8	127.4
C_α−C_β−H	124.2	123.9	124.5	124.5	
(C_α−C_β−H)[a]	125.3	125.2	125.5	125.6	
C_α−C_m−H	117.0	116.8	116.1	116.0	
C_β−C_β−H	127.7				
(C_β−C_β−H)[a]	128.5				

[a] For bonds belonging to the unprotonated pyrrole rings.

Results and Discussion

The atomic definitions for FBP were taken according to Zgierski's notations[16] with C_α, C_β, and C_m being the carbon atoms in the α, β, and meso positions. The optimized structure obtained on the isolated molecule using the DFT method is in good agreement with the results of X-ray studies,[17] and this fact shows that only weak distortions would appear in the crystal state (Table 2).

The optimized parameters are compared in Table 2 to other theoretical values obtained from studies using the LDFT, SCF/TZDP, and MP2/DZP2 methods.[18,20] It can be easily seen that the calculated values are in quite agreement with the experimental ones, the mean deviations being 0.005 Å for bonds and 1.3° for angles.

Table 3 displays a set of scaling factors referring to different groups of internal coordinates. Ten different values were retained after the fitting of the theoretical wavenumbers to the experimental ones. Their values lie in the 0.92−0.98 range except for those corresponding to the NH stretching value which displays a lower value (0.87). The derived diagonal force constants expressed in the internal coordinate space are displayed in Table 4.

These scaling factors have to be compared to the corresponding values given in ref 5. The N−C and C−C stretchings coordinates have a calculated value of 0.93, which is to be compared to the value of 0.927 obtained in this work. The values

TABLE 3: Calculated Scaling Factors for Force Constants According to the Different Groups of Internal Coordinates (IC)

IC	in plane	scaling factor	IC	out of plane	scaling factor
R1,R2	NH	0.8695	R111,R112	NH opb	0.95
R3,R6	C_mH	0.9165	R113,R116	C_mH opb	0.92
R7,R14	$C_\beta H$	0.9165	R117,R124	$C_\beta H$ opb	0.92
R15,R22	NC	0.927	R125,R132	$C_\alpha C_m$opb	0.99
R23,R30	C_mC_α	0.927	R133,R140	NCtor	0.95
R31,R38	$C_\beta C_\alpha$	0.927	R141,R148	$C_mC_\alpha$tor	0.935
R39,R42	$C_\beta C_\beta$	0.927	R149,R156	$C_\beta C_\alpha$tor	0.935
R43,R46	CNH	0.952	R157,R160	$C_\beta C_\beta$tor	0.935
R47,R54	$C_\alpha C_mH$	0.952			
R55,R62	$C_\alpha C_\beta H$	0.952			
R63,R70	$C_\beta C_\beta H$	0.952			
R71,R74	CNC	0.98			
R75,R82	$NC_\alpha C_m$	0.98			
R83,R90	$NC_\alpha C_\beta$	0.98			
R91,R98	$C_mC_\alpha C_\beta$	0.98			
R99,R102	$C_\alpha C_mC_\alpha$	0.98			
R103,R110	$C_\alpha C_\beta C_\beta$	0.98			

TABLE 4: Scaled General Valence Diagonal Force Constants Obtained for FBP

IC[a]	bond stretching (mdyn/Å)	IC[a]	angle bending (mdyn Å)
N−H	6.21	H−N−C_α	0.38
N−C_α	4.12	C_α−N−C_α	0.74
(N−C_α)[b]	3.95	(C_α−N−C_α)[b]	1.10
C_β−C_α	3.66	N−C_α−C_β	0.72
(C_β−C_α)[b]	3.25	(N−C_α−C_β)[b]	0.75
C_β−C_β	4.90	C_α−C_β−C_β	0.7
(C_β−C_β)[b]	5.52	(C_α−C_β−C_β)[b]	0.68
C_m−C_α	6.28	N−C_α−C_m	0.527
(C_m−C_α)	6.06	(N−C_α−C_m)[b]	0.59
C_β−H	5.27	C_α−C_m−C_α	0.526
(C_β−H)[b]	5.27	C_α−C_β−H	0.396
C_m−H	5.13	(C_α−C_β−H)[b]	0.38
		C_α−C_m−H	0.4
		C_β−C_β−H	0.38
		(C_β−C_β−H)[b]	0.38

[a] IC: internal coordinate. [b] For bonds belonging to the unprotonated pyrrole rings.

for the C−H stretching given our work and in the reference[5] are in good agreement (0.916 and 0.912, respectively). The values for the N−H rocking in-plane coordinate are comparable (0.95 and 0.94), and likewise values corresponding to the out of plane wagging (0.95 and 9486). A discrepancy can be noted for the in-plane CH deformation (0.952 and 0.934). The scaling factors applying to the ring stretching coordinates have quite comparable values: 0.98 (this work) and 0.988.[5]

No great differences between the scaling factors can be noted when one uses a set of redundant or nonredundant internal coordinates.

Vibrational Analysis. The calculated frequencies and normal mode symmetries (D_{2h} molecular geometry) for FBP are given in Table 5. Only the highest contributions to the potential energy distribution (PED) among the internal coordinates were reported.

The theoretical wavenumbers for the d_0, d_2(NH), d_4(C_mH), d_8($C_\beta H$), and d_{12}(C_mH,$C_\beta H$) isotopomers are compared to their corresponding experimental values[4,5] in Table 6. It is noteworthy that the same set of scaling factors was kept for the five isotopomers.

In refs 4 and 5 a particular detailed analysis of the vibrational (infrared and nonresonant Raman) activities was performed and a correlation was established between some of them and their appearance in the fluorescence and phosphorescence emissions according to their symmetry properties. The present work was done using the same basis and correlation functions as in ref 4. It can be easily deduced from Tables 5 and 6 that the calculated wavenumbers and PED for all the isotopomers are quite in correspondence with the experimental bands. The assignments for the d_2, d_4, d_8, and d_{12} analogues were done according to their potential energy distribution. Only a few calculated frequencies are in disagreement with the previous assignments. In particular, the calculated wavenumber at 776 cm^{-1} for the B_{1u} mode (D_{2h}) in the d_2 isotopomer corresponds to the observed band at 785 cm^{-1} in d_0. For this band, Kozlowski et al.[4,5] discussed the validity of the calculated dipole moments and preferred to assign the d_2 wavenumber at 535 cm^{-1}. This explanation is somewhat difficult to understand since the potential energy distribution for the d_0 and d_2 isotopomers does not show any participation of the C_αNH group to this mode (no shift) and any dependence on the type of basis sets.

Resonance Raman Intensities. *Simplified Theory for the Resonance Raman Intensities.* For molecules containing π-electron conjugated systems, the first allowed electronic transitions are generally of the $\pi \rightarrow \pi^*$ type. Along these electronic transitions, some normal modes can be perturbed by the changes occurring in the molecular geometry and electronic bonding. Such changes principally affect the atomic equilibrium displacements in the excited electronic state with respect to the ground state. To follow such geometrical perturbations, the vibrational analysis appears to be a powerful method to investigate the changes taking place in the atomic distances and valence angles. Wilson's *GF* method[21] was until now extensively used to deal with the normal modes determination as its relates the internal coordinates R (stretching, in-plane and out-of-plane bending, torsion) to the $3N - 6$ normal coordinates Q_i of a molecule containing N atoms according to the matrix relation $Q = L^{-1}R$. In this last formulation, L stands for the eigenvector matrix that can be derived from the resolution of the well-known relationship $GFL = L\Lambda$, where G and F represent the inverse kinetic energy and potential energy matrices, respectively. The matrix of internal coordinates R can be obtained from the $3N$ Cartesian coordinates via the B matrix involving the Wilson's vectors and the relationship $R = BX$. Along an electronic transition, the variations ΔR occurring in the internal coordinates are related to the shifts in the normal coordinates ΔQ according to the following expression: $\Delta Q = L^{-1}(\Delta R) = L^{-1}B(\Delta X)$.

Using quantum mechanical methods (semiempirical or ab initio) it is relatively easy to calculate the bond lengths and bond angles of a molecule at its potential energy minimum for the ground and excited electronic states. From this, it is possible to deduce the displacements of the potential energy minimum along some particular normal modes from those occurring in the internal coordinates. It has been suggested that the changes in bond lengths Δr_i along a particular electronic transition are proportional to the corresponding changes (Δbo) of the bond orders; i.e., $\Delta R_i = C(\Delta \mathrm{bo})_i$, where the subscript i corresponds to the ith bond and C is a constant. For molecules having totally symmetric modes, the main origin of the resonance Raman enhancements arises from the A term of the scattering tensor and the associated intensity I_j of the jth normal mode can be shown to be approximatively proportional to the square of the shift ΔQ_j appearing along this normal mode between the ground and the excited electronic state; i.e., $I_j = K(\Delta Q_j)^2 \nu_j^2$, where ν_j refers to the associated linear frequency of the normal mode.[9,22,23] Then, considering the linear relationship between the kth change in bond length and its associated change in bond order, the resonance Raman intensity of the jth normal mode is given by

$$I_j = CK\nu_j^2 \sum_k (L_k^{-1})(\Delta \mathrm{bo}_k)^2$$

TABLE 5: Wavenumbers and Potential Energy Distribution for the d_0 Isotopomer of FBP (D_{2h}) Obtained after Scaling of the Force Constant[a]

no.	sym	calc	PED	no.	sym	calc	PED
1	B_{1u}	51.7	39τNC, 17τC_mC_α, 10$\tau C_\beta C_\alpha$, 27πC_mC_α	57	B_{2u}	981.7	53$\nu C_\beta C_\alpha$, 15νCN
2	B_{1g}	72.3	29δCNH, 24$\delta C_\alpha C_mC_\alpha$, 18$\delta NC_\alpha C_m$, 16$\delta C_mC_\alpha C_\beta$	58	A_g	984.5	35νCN, 16$\nu C_\beta C_\alpha$, 14$\delta HC_\beta C_\alpha$, 14δHNC
3	A_u	92.0	38τC_mC_α, 25πC_mH, 21πC_mC_α	59	B_{3u}	1002.4	30$\nu C_\beta C_\alpha$, 20νCN, 17$\delta HC_\beta C_\alpha$
4	B_{1u}	117.8	35τC_mC_α, 28πC_mC_α, 14πC_mH, 11πNH	60	B_{1g}	1004.4	23$\nu C_\beta C_\alpha$, 16νCN, δHNC
5	B_{2g}	135.1	69τC_mC_α, 16πNH, 16πC_mC_α	61	B_{2u}	1052.1	45$\delta HC_\beta C_\beta$, 39$\delta HC_\beta C_\alpha$
6	B_{3g}	138.1	59τC_mC_α, 16πC_mC_α, 14πC_mH	62	B_{3u}	1053.5	39$\delta HC_\beta C_\beta$, 32$\delta HC_\beta C_\alpha$
7	A_g	160.9	42$\delta NC_\alpha C_m$, 40$\delta C_mC_\alpha C_\beta$	63	A_g	1054.9	44$\delta HC_\beta C_\beta$, 38$\delta HC_\beta C_\alpha$
8	B_{2g}	192.4	32πC_mC_α, 22$\tau C_\beta C_\alpha$, 17τNC, 14τC_mC_α	64	A_g	1063.7	44$\delta HC_\beta C_\beta$, 37$\delta HC_\beta C_\alpha$
9	B_{3g}	212.6	50τC_mC_α, 22πNH, 14πC_mC_α	65	B_{1g}	1132.6	27νCN, 13νC_mC_α, 10$\nu C_\beta C_\alpha$, 19δHC_mC_α
10	B_{1u}	213.5	36πC_mC_α, 27τNC, 16τC_mC_α, 16$\tau C_\beta C_\alpha$	66	B_{3u}	1136.0	32νCN, 12$\nu C_\beta C_\alpha$, 9νC_mC_α
11	B_{2u}	290.2	40$\delta NC_\alpha C_m$, 36$\delta C_mC_\alpha C_\beta$	67	B_{2u}	1155.1	17νCN, 15$\nu C_\beta C_\alpha$, 26δHC_mC_α, 14$\delta HC_\beta C_\alpha$, 10$\delta HC_\beta C_\beta$
12	A_u	296.0	45πC_mC_α, 25$\tau C_\beta C_\alpha$, 18τNC				
13	A_g	301.3	41νC_mC_α, 11$\nu C_\beta C_\alpha$, 10$\delta C_\alpha C_mC_\alpha$	68	A_g	1177.7	26$\nu C_\beta C_\alpha$, 15CN, 35δHC_mC_α, 10δCNC
14	B_{3u}	310.5	36$\delta C_mC_\alpha C_\beta$, 35$\delta NC_\alpha C_m$	69	B_{1g}	1183.9	20νC_mC_α, 11$\nu C_\beta C_\alpha$, 10νCN, 21$\delta HC_\beta C_\beta$, 20$\delta HC_\beta C_\alpha$, 10δHC_mC_α
15	B_{1u}	331.8	42τC_mC_α, 16τNC, 14$\tau C_\beta C_\alpha$				
16	B_{3u}	344.0	36νC_mC_α, 12$\nu C_\beta C_\alpha$, 18$\delta C_mC_\alpha C_\beta$	70	B_{1g}	1225.9	33νC_mC_α, 47δHNC
17	B_{2u}	347.8	37νC_mC_α, 12$\nu C_\beta C_\alpha$, 19$\delta C_mC_\alpha C_\beta$	71	B_{3u}	1226.6	24νC_mC_α, 24νCN, 12$\nu C_\beta C_\alpha$
18	B_{1g}	389.9	45$\delta NC_\alpha C_m$, 45$\delta C_mC_\alpha C_\beta$	72	B_{2u}	1226.9	12νC_mC_α, 51δHNC
19	B_{1g}	407.8	35νC_mC_α, 19$\nu C_\beta C_\alpha$, 24$\delta C_mC_\alpha C_\beta$	73	B_{2u}	1254.6	12νCN, 9$\nu C_\beta C_\alpha$, 13$\delta HC_\beta C_\alpha$, 12δHC_mC_α, 11$\delta HC_\beta C_\beta$
20	B_{2g}	419.3	25τC_mC_α, 18$\tau C_\beta C_\alpha$, 14πC_mC_α, 10πNH, 10πC_mH				
21	B_{3g}	430.0	26τC_mC_α, 18$\tau C_\beta C_\alpha$, 16τNC, 16πC_mC_α, 12πC_mH	74	B_{3u}	1289.6	20νC_mC_α, 12$\nu C_\beta C_\alpha$, 26$\delta HC_\beta C_\beta$, 12$\delta HC_\beta C_\alpha$
22	A_u	470.0	25τC_mC_α, 21$\tau C_\beta C_\alpha$, 10τNC, 11πC_βH, 20πC_mH	75	B_{1g}	1322.2	31νCN, 14νC_mC_α, 14$\delta HC_\beta C_\beta$
23	B_{2g}	605.0	51πNH, 36τNC	76	A_g	1351.5	34$\nu C_\beta C_\alpha$, 16νCN, 11δCNC
24	B_{1u}	642.3	43πC_mC_α, 27πNH, 12πC_βH	77	B_{1g}	1356.7	27$\delta HC_\beta C_\beta$, 20$\delta HC_\beta C_\alpha$, 20δHC_mC_α
25	B_{2g}	665.8	63πC_mC_α, 17πC_βH	78	B_{2u}	1358.8	21νCN, 20$\nu C_\beta C_\alpha$, 19$\delta HC_\beta C_\beta$
26	B_{3g}	667.4	68πC_mC_α, 13τNC	79	B_{1g}	1381.0	28νCN, 25$\nu C_\beta C_\alpha$, 13$\delta HC_\beta C_\beta$
27	A_u	675.7	72πC_mC_α, 11$\tau C_\beta C_\beta$	80	A_g	1398.9	28νCN, 15$\nu C_\beta C_\alpha$, 16$\nu C_\beta C_\beta$, 24δHC_mC_α
28	B_{2g}	695.5	66πC_mC_α, 19τC_mC_α	81	B_{3u}	1399.7	27$\nu C_\beta C_\beta$, 22νCN, 10$\nu C_\beta C_\alpha$, 20δHC_mC_α
29	A_u	695.8	62πC_mC_α, 18τC_mC_α	82	B_{2u}	1406.3	30νCN, 12$\nu C_\beta C_\beta$, 24δHC_mC_α
30	B_{1u}	697.3	47πC_mC_α, 24πC_βH	83	B_{3u}	1413.0	35$\nu C_\beta C_\alpha$, 19νC_mC_α
31	B_{3g}	700.0	51πC_mC_α, 20πC_βH	84	A_g	1424.3	30νC_mC_α, 39$\nu C_\beta C_\beta$, 15νCN
32	A_g	719.2	22νCN, 11νC_mC_α, 14$\delta NC_\alpha C_m$	85	B_{1g}	1495.1	38νC_mC_α, 13CN, 10HC_mC_α
33	A_g	722.7	21νC_mC_α, 21$\delta NC_\alpha C_\beta$, 18δCNC, 14$\delta C_mC_\alpha C_\beta$	86	B_{2u}	1497.1	21$\nu C_\beta C_\beta$, 17νC_mC_α, 12νCN, 12δHNC
34	B_{3u}	731.8	30πC_βH, 11πC_mC_α	87	A_g	1508.5	48$\nu C_\beta C_\beta$, 15$\delta HC_\beta C_\alpha$
35	B_{3u}	734.0	20νC_mC_α, 11νCN, 12$\delta NC_\alpha C_\beta$, 12$\delta C_mC_\alpha C_\beta$	88	B_{3u}	1516.8	53νC_mC_α
36	B_{2u}	744.0	14νC_mC_α, 9νCN, 14$\delta NC_\alpha C_\beta$, 13$\delta C_mC_\alpha C_\beta$, 9$\delta$CNC	89	B_{3u}	1528.4	29νC_mC_α, 27$\nu C_\beta C_\beta$, 16 δHC_mC_α
37	B_{3g}	764.3	56πC_βH, 21πC_mC_α	90	B_{2u}	1548.5	28νC_mC_α, 28$\nu C_\beta C_\beta$, 10$\delta HC_\beta C_\alpha$
38	B_{2g}	771.5	51πC_βH, 20πC_mC_α	91	A_g	1559.7	35$\nu C_\beta C_\beta$, 18νC_mC_α, 12$\delta HC_\beta C_\alpha$
39	B_{1u}	772.1	61πC_βH, 8πC_mC_α	92	B_{1g}	1592.0	57νC_mC_α, 9δHC_mC_α
40	B_{1g}	780.9	25$\delta C_\alpha C_\beta C_\beta$, 13$\delta C_\alpha C_mC_\alpha$, 12$\delta NC_\alpha C_\beta$, 11$\delta NC_\alpha C_m$	93	B_{2u}	1596.4	57νC_mC_α, 9δHC_mC_α
41	B_{2u}	784.2	10$\nu C_\beta C_\alpha$, 25$\delta C_\alpha C_\beta C_\beta$, 18$\delta NC_\alpha C_\beta$	94	A_g	1600.8	74νC_mC_α, 12δHC_mC_α
42	B_{1u}	785.4	42πC_βH, 24πNH	95	B_{1g}	3056.3	98νC_mH
43	B_{3u}	787.9	16νC_mC_α, 26$\delta C_\alpha C_\beta C_\beta$, 12$\delta C_\alpha C_mC_\alpha$, 10$\delta NC_\alpha C_\beta$	96	A_g	3057.7	99νC_mH
44	B_{1g}	806.2	28$\delta C_\alpha C_\beta C_\beta$, 12$\delta C_\alpha C_mC_\alpha$, 10$\delta NC_\alpha C_\beta$, 12$\delta NC_\alpha C_m$	97	B_{3u}	3057.8	98νC_mH
45	B_{3g}	839.0	63πC_mH, 18τC_mC_α	98	B_{2u}	3058.7	99νC_mH
46	A_u	840.0	64πC_mH, 17τC_mC_α	99	B_{1g}	3090.5	98νC_mH
47	B_{2g}	845.0	62πC_mH, 17τC_mC_α	100	B_{3u}	3090.7	98νC_βH
48	B_{1u}	845.6	61πC_mH, 16τC_mC_α	101	B_{2u}	3106.8	98νC_βH
49	A_u	882.4	54πC_βH, 27$\pi C_\beta C_\beta$	102	B_{1g}	3107.2	98νC_βH
50	B_{2g}	883.7	60πC_βH, 26$\pi C_\beta C_\beta$	103	B_{2u}	3107.4	98νC_βH
51	B_{3g}	890.1	44πC_βH, 26$\pi C_\beta C_\beta$, 18πC_mH	104	A_g	3109.2	98νC_βH
52	A_u	891.1	45πC_βH, 24$\pi C_\beta C_\beta$, 18πC_mH	105	B_{3u}	3116.7	98νC_βH
53	A_g	947.7	52$\nu C_\beta C_\alpha$, 16νCN	106	A_g	3123.6	98νC_βH
54	B_{2u}	948.7	45$\nu C_\beta C_\alpha$, 15νCN	107	B_{3u}	3328.7	100νNH
55	B_{1g}	969.5	32νCN, 11$\nu C_\beta C_\alpha$, 22δHNC, 13$\delta HC_\beta C_\alpha$	108	A_g	3367.3	100νNH
56	B_{3u}	971.2	46$\nu C_\beta C_\alpha$, 18νCN				

[a] Abreviations used: ν, stretching; δ, in-plane bending; π, out-of-plane bending; τ, torsion.

If one gives a value of 10 to the most intense band, one can calculate the other relative resonance Raman intensities for a particular electronic transition. It can be shown from the above simplified equations that the most intense enhancements will be given by the normal modes that contain bonds which are specifically affected by the electronic transition under consideration. A force field leading to erroneous enhancements would have to be rejected because the potential energy distribution would contain wrong combinations of the internal coordinates.

Results. Several resonance Raman spectra on the free base porphine (FBP) and of some of its substitued analogues have been reported[1,2] for the first electronic transitions. The understanding of the composition of the excited states of the free base porphine would be essential to study the electronic changes occurring under photoexcitation or interactions with external electrons particularly in the case of biological reactions. Among recent studies on the electronic properties of the free base porphine, Nakatsuji et al.[24] reported a SAC-CI study on the ground, excited, and ionized states of free base porphine The infrared, Raman, resonance Raman, fluorescence, and phosphorescence properties have been also investigated in an extensive way and compared to theoretical vibrational analyses via a scaled quantum mechanical study.[4,5]

FBP has a D_{2h} symmetry which can was correlated to the D_{4h} of the metalloporphyrins. Nakatsuji et al.[24] using SAC-CI treatments have shown that Gouterman's four orbital model[25] perfectly explains the ground-state electronic state of the FBP and that these orbitals are all of the π type, i.e., Homo $-$ 1,

TABLE 6: Experimental and Calculated Wavenumbers (in cm^{-1}) for the d_0, d_2, d_4, d_8, and d_{12} Isotopomers

		d_0		d_2		d_4		d_8		d_{12}				d_0		d_2		d_4		d_8		d_{12}	
no.	sym	exp	calc	exp	calc	exp	calc	exp	calc	exp	calc	no.	sym	exp	calc	exp	calc	exp	calc	exp	calc	exp	calc
1	B_{1u}		51.7		51.7		52		50		50	55	B_{1g}	976	969.5		861	972	976	846	843	840	837
2	B_{1g}	109	72.3		71.2		72		72		71	56	B_{3u}	971	971.2	957	954	981	978	773	780	775	758
3	A_u		92.0		92.1		89		90		87	57	B_{2u}	977	981.7		865	961	954	784	781		767
4	B_{1u}		117.8		116.1		117		111		111	58	A_g	988	984.5	978	968		956.2	794	792	770	771
5	B_{2g}		135.1		131.1		135		128		128	59	B_{3u}	994	1002.4		1002		924	884	885		872
6	B_{3g}		138.1		138.1		137		131		130	60	B_{1g}	1005	1004.4	1004	1004	998	1001	908	910	896	897
7	A_g	155	160.9	155	160.3	155	160.8	153	158.3	152	158.3	61	B_{2u}	1054	1052.1	1053	1051	996	992	881	879	870	868
8	B_{2g}		192.4		191.4		186		188		182	62	B_{3u}	1043	1053.5	1043	1053	1044	1055	959	958	920	926
9	B_{3g}		212.6		211.7		212		207		207	63	A_g	1063	1054.9	1056	1055	1015	1007	944	937	923	921
10	B_{1u}	219	213.5		213.5		208		208		203	64	A_g	1064	1063.7	1062	1063	1072	1061	978	967.6	957	947
11	B_{2u}		290.2		282.2		290		282		279	65	B_{1g}	1138	1132.6	1182	1186	918	924	1095	1094	928	922
12	A_u		296.0		296		296		277		277	66	B_{3u}	1134	1136.0	1134	1135	990	1002	1092	1087	969	967
13	A_g	309	301.3	308	300	308	300.8	303	295.3	302	294.8	67	B_{2u}	1156	1155.1	1098	1095	1062	1058		1063	952	950
14	B_{3u}	310	310.5		309.5		306		303		299	68	A_g	1172	1177.7	1175	1175	1072	1071.4	1171	1173	1019	1008.5
15	B_{1u}	335	331.8		332		304		328		301	69	B_{1g}	1182	1183.9		1157	1170	1159	1045	1042	1043	1040
16	B_{3u}	357	344.0		343.3		343		324		323	70	B_{1g}	1226	1225.9		1094	1218	1212	1218	1217	1149	1151
17	B_{2u}	357	347.8		347.3	357	346		330		329	71	B_{3u}	1177	1226.6	1172	1166	1161	1199	1162	1209	1114	1132
18	B_{1g}	389	389.9	389	383	384	383	372	371	363	365	72	B_{2u}	1228	1226.9		1223	1203	1208	1204	1204		1111
19	B_{1g}	418	407.8	418	407.7	419	408	389	376	385	376	73	B_{2u}	1255	1254.6	1255	1252	1241	1239	1225	1229	1211	1212
20	B_{2g}		419.3		418.7		402		395		379	74	B_{3u}	1287	1289.6		1289	1264	1275	1210	1218	1173	1228
21	B_{3g}		430.0		430		410		408		388	75	B_{1g}	1313	1322.2	1316	1322	1290	1294	1238	1240	1282	1290
22	A_u		470.0		470		454		434		422	76	A_g	1352	1351.5		1349	1318	1316.0	1349	1341	1316	1319
23	B_{2g}		605.0		454.4		618		543		542	77	B_{1g}	1350	1356.7	1362	1355	1331	1334	1315	1321	1230	1213
24	B_{1u}	639	642.3		651		626		541		541	78	B_{2u}	1357	1358.8	1352	1356	1339	1341	1324	1320	1310	1313
25	B_{2g}		665.8		665.8		677		549		549	79	B_{1g}	1400	1381.0	1385	1379	1388	1377	1364	1363	1355	1341
26	B_{3g}		667.4		538		669		643		632	80	A_g	1384	1398.9		1393	1364	1368.2	1401	1399	1359	1356
27	A_u		675.7		675.7		678		610		611	81	B_{3u}	1396	1399.7	1394	1394	1352	1377	1359	1354	1350	1347
28	B_{2g}		695.5		695.6		646		559		559	82	B_{2u}	1406	1406.3		1398	1347	1359	1402	1400	1352	1360
29	A_u		695.8		695.7		594		656		587	83	B_{3u}	1412	1413.0	1406	1412	1409	1412	1406	1395	1369	1374
30	B_{1u}	691	697.3	693	697.3	647	731	566	622	563	594	84	A_g	1424	1424.3	1428	1424	1428	1417.1	1405	1404	1398	1396.0
31	B_{3g}		700.0		700		714		622		600	85	B_{1g}	1493	1495.1	1493	1484	1480	1480	1478	1484	1466	1468
32	A_g	723	719.2	721	719	663	662	701	697.2	665	653	86	B_{2u}	1490	1497.1	1479	1480	1479	1487	1447	1463	1447	1452
33	A_g	736	722.7	726	721.1	702	697	722	715	699	695	87	A_g	1492	1508.5	1496	1508	1485	1497	1450	1463	1451	1455
34	B_{1u}	731	731.8		657	699	701		703	635	629	88	B_{3u}	1507	1516.8		1517	1498	1503		1493	1471	1477
35	B_{3u}	723	734.0	723	733	680	687	700	704	667	672	89	B_{3u}	1522	1528.4		1527	1505	1517	1515	1518	1500	1497
36	B_{2u}	745	744.0	744	731	694	693		761	677	676	90	B_{2u}	1540	1548.5		1548	1542	1545	1521	1525	1522	1519
37	B_{3g}		764.3		758		776		731		733	91	A_g	1544	1559.7	1555	1559	1554	1555.7	1524	1528.3	1518	1522.1
38	B_{2g}		771.5		764		788		707		652	92	B_{1g}		1592.0	1590	1582	1587	1581	1594	1587	1579	1575
39	B_{1u}	773	772.1	762	769	745	752	722	721	709	706	93	B_{2u}		1596.4		1586		1587		1590		1580
40	B_{1g}	786	780.9		746	763	761	758	755	747	743	94	A_g	1609	1600.8	1614	1601	1601	1587.2	1615	1598.6	1598	1585
41	B_{2u}		784.2		740		768	710	709	752	751	95	B_{1g}		3056.3	3041	3056	2263	2256.9		3057	2258	2256.4
42	B_{1u}	785	785.4		776	779	774	753	759	745	742	96	A_g		3057.7	3059	3058		2257.6		3058		2257.1
43	B_{3u}	780	787.9		787	770	776	760	760	741	749	97	B_{3u}	3042	3057.8	3042	3058	2266	2257.7	3040	3058	2260	2257.6
44	B_{1g}	805	806.2	805	800	796	793	776	773	762	760	98	B_{2u}	3045	3058.7	3045	3059	2258	2257.7	3046	3059	2258	2257.6
45	B_{3g}		839.0		839		744		849		679	99	B_{1g}		3090.5		3090		3090.2		2280.2		2280.6
46	A_u		840.0		840		619		846		653	100	B_{3u}	3088	3090.7	3118	3091		3090.4		2280.4	2269	2280.8
47	B_{2g}		845.0		845		598		842		723	101	B_{2u}	3112	3106.8	3112	3107	3110	3107.0		2296.5	2263	2296.6
48	B_{1u}	852	845.6	853	846	799	794	847	839	764	759	102	B_{1g}		3107.2		3107		3107.2		2296.6		2296.7
49	A_u		882.4		882		882		742		747	103	B_{2u}	3124	3107.4	3124	3108	3122	3107.4	2338	2321.4	2324	2321.4
50	B_{2g}		883.7		884		882		732		761	104	A_g		3109.2		3109		3109.2		2322.6		2322.6
51	B_{3g}		890.1		890		888		738		760	105	B_{3u}	3128	3116.7	3128	3117	3117	3116.9	2336	2323.5	2334	2323.5
52	A_u		891.1		891		888		729		767	106	A_g	3158	3123.6		3124		3123.6		2328.8		2328.5
53	A_g	952	947.7	950	946	920	914.0	776	767	773	762	107	B_{3u}	3324	3328.7	2475	2449	3324	3328.7	3324	3328.7		3328.7
54	B_{2u}	951	948.7	950	948	923	923	938	935	918	920	108	A_g		3367.3		2474		3367.3		3367.3		3367.3

Homo, Lumo, and Lumo + 1. They have shown that these molecular orbitals (MO) display π conjugation over the whole molecule and noted that an another MO of the π type could strongly perturbe this model.

The lowest energetic electronic transitions are given by two pairs of degenerate states the Q bands (Q_x, Q_y) and the B_x (B Soret band) and N states lying respectively at 480 and 380 nm in the electronic spectrum of the FBP. The components of each pair are polarized perpendicularly to the components of the other pair.

In the resonance Raman spectra, the totally symmetric A_g modes (for FBP with D_{2h} symmetry) will be enhanced via two kinds of mechanisms: (i) the Frank−Condon (FC) mechanism (which originates in the difference between the equilibrium geometries of the ground and excited electronic states; (ii) the Herzberg−Teller (HT) mechanism (vibronic coupling between electronic states). The relative enhancements observed for the electronic transition centered on the Q band have been given in ref 2.

The FC mechanism will lead to polarized Raman bands with a polarization ratio lying in the 0.125 and 0.75 range. The Raman bands originating from the HT coupling generally give depolarized bands ($\rho = 0.75$), but in the case of two excited states belonging to the same representation their direct product containing the totally symmetric representation can lead to the appearance of a nonzero (resonance) Raman activity.

In the present work, we tried to use a DFT description of the frontier orbitals to give a crude description of the resonance activity for the lowest electronic transitions.

For the free base porphine with D_{2h} symmetry, Table 7 gives the eigenvalues and symmetries of the molecular orbitals together with values obtained from other studies.[24,26,27] In the

TABLE 7: Eigenvalues (in eV) and Symmetries of the Frontier Orbitals As Obtained from Different Quantum Mechanical Studies

molecular orbital	DFT/B3-LYP (this work)		LDA[26]		CAS-SCF[27]		SAC-CI[24]	
	energy	sym	energy	sym	energy	sym	energy	sym
Lumo + 2			−0.58	A_u (π)				
Lumo + 1	−2.23	B_{2g} (π)	−1.92	B_{3g} (π)	3.06	B_{2g} (π)	0.141	$4b_{3g}$
Lumo	−2.24	B_{3g} (π)	−1.94	B_{2g} (π)	2.88	B_{3g} (π)	−0.069	$4b_{2g}$
Homo	−5.16	B_{1u} (π)	−3.90	B_{1u} (π)	−4.18	A_u (π)	−6.52	2au
Homo − 1	−5.30	A_u (π)	−4.15	A_u (π)	−4.24	B_{1u} (π)	−6.68	$5b_{1u}$
Homo − 2			−4.71	B_{2g} (π)	−7.10			
Homo − 3			−4.84	B_{1u} (π)				
Homo − 4			−5.17	Ag (σ)				
Homo − 5			−5.19	B_{3u} (σ)				

TABLE 8: Molecular Orbital Coefficients Occurring in the Frontier Orbitals of FBP As Estimated from the Ground State[a]

atom numbering	basis function	Homo − 1 (−0.194 819 E_h, OCC 1, sym A_u)	Homo (−0.189 607 E_h, OCC 1, sym B_{1u})	Lumo (−0.082 385 E_h, OCC 0, sym B_{3g})	Lumo + 1 (−0.081 991 E_h, OCC 0, sym B_{2g})
N1	3s		0.212	−0.175	
	$2p_x$		0.176	−0.170	
N3	3s		0.212	0.175	
	$2p_x$		0.176	0.170	
N6	3s	0.146			0.157
	$2p_x$	0.138			0.172
N7	3s	0.146			−0.157
	$2p_x$	0.138			−0.172
C8	3s	0.191	−0.065	0.138	0.113
	$2p_x$	0.142	−0.041	0.127	0.110
C9	3s	−0.191	−0.065	−0.138	0.113
	$2p_x$	−0.142	−0.041	−0.127	0.110
C10	3s	0.199		0.065	−0.167
	$2p_x$	0.144		0.050	−0.146
C11	3s	−0.199		0.065	−0.167
	$2p_x$	−0.144		0.050	−0.146
C12	3s	0.191	−0.065	−0.138	−0.113
	$2p_x$	0.142	−0.041	−0.127	−0.110
C13	3s	−0.191	−0.065	0.138	−0.113
	$2p_x$	−0.142	−0.041	0.127	−0.110
C14	3s	0.199		−0.065	0.167
	$2p_x$	0.144		−0.050	0.146
C15	3s	−0.199		−0.065	−0.167
	$2p_x$	−0.144		−0.050	−0.146
C17	3s			0.045	−0.153
	$2p_x$			0.038	−0.158
C18	3s		−0.229	−0.193	0.159
	$2p_x$		−0.199	−0.190	0.145
C19	3s	0.108	0.073	0.165	0.070
	$2p_x$	0.096	0.057	0.167	0.069
C20	3s		−0.229	0.193	0.159
	$2p_x$		−0.199	0.190	0.145
C21	3s	0.095		0.045	0.53
	$2p_x$	0.088		0.038	0.158
C22	3s		−0.229	−0.165	−0.159
	$2p_x$		−0.199	−0.190	−0.145
C23	3s	−0.108	0.073	0.165	0.070
	$2p_x$	−0.096	0.057	0.167	0.069
C24	3s	0.095		−0.045	−0.153
	$2p_x$	0.088		−0.038	−0.158
C26	3s		−0.229	0.193	−0.159
	$2p_x$		−0.199	0.190	−0.145
C27	3s	0.108	0.073	−0.165	0.070
	$2p_x$	0.096	0.057	−0.167	0.069
C28	3s	−0.108	0.073	−0.165	−0.070
	$2p_x$	−0.096	0.057	−0.167	0.069
C29	3s	−0.095		−0.045	0.153
	$2p_x$	−0.088		−0.038	0.158

[a] Molecular orbital energies are expressed in hartrees (E_h). OCC and sym are the occupancy number and symmetry type, respectively.

present work, the excitation energies for the Homo to Lumo (H → L), Homo to Lumo + 1 (H → L + 1), Homo − 1 to Lumo (H − 1 → L), and H − 1 → L + 1 transitions have been calculated to correspond to the 425−405 nm range.

Nakatsuji et al.[24] have shown that the Q band is composed of two bands (Q_x and Q_y) assigned to the $1B_{3u}$ and $1B_{2u}$ states, respectively, and noted an overestimation of 0.2 eV in the corresponding excitation energies. If one takes the same relative error for the excitation energy, the electronic transition obtained from the present DFT study would be centered at about 450 nm and related to the Q electronic band.

Table 8 displays the molecular orbital coefficients (MOC) calculated for the ground state of FBP (D_{2h} symmetry). The most important contributions to the MOC are given by the Rydberg (3s) orbitals that are very poorly occupied and by the $2p_z$ coefficients (with z being perpendicular to the molecular

TABLE 9: Changes in the Bond Orders Occurring in the Electronic Transitions Represented by the Four-Orbital Model

internal coord	Δbo- (H → L)	Δbo- (H → L + 1)	Δbo- (H − 1 → L)	Δbo- (H − 1 → L + 1)
N−H	0.0000	0.0000	0.0000	0.0000
C_m-C_α	−1.1791	2.5329	−0.4849	3.1883
$(C_m-C_\alpha)^a$	1.0231	−1.9433	1.4258	−1.5034
C−N	−0.4593	−1.9237	−0.9042	−2.3503
$(C-N)^a$	−0.5519	0.1806	−0.3568	0.3665
$C_\beta-C_\alpha$	1.6846	−0.8661	2.7476	0.2287
$(C_\beta-C_\alpha)^a$	−0.1734	2.0333	1.0091	3.1883
$C_\beta-C_\beta$	−2.0930	0.8391	−2.5419	0.3535
$(C_\beta-C_\beta)^a$	0.1661	−2.2313	−0.5435	−2.9111
C_m-H	0.0000	0.0000	0.0000	0.0000
$C_\beta-H$	0.0000	0.0000	0.0000	0.0000

[a] For bonds belonging to the unprotonated pyrrole rings.

plane). The four orbitals are all of the π type and correspond to the description of Gouterman.[25]

Table 9 gives the calculated bond order changes for the monoelectronic H → L transition and for the other possible transitions. As the bond order changes are opposed in sign to the changes in bond lengths, the π bond lengths decrease while the σ bond lengths increase and the relative changes in bond orders follow the totally symmetric representation. The most intense changes in bond orders are given for the four molecular orbitals by the $C_\beta{=}C_\beta$ and $C_\alpha-C_\beta$ bonds in the protonated pyrrole rings.

Table 10 gives the predicted resonance Raman intensities (RRI) for the normal modes belonging to the A_g species. The RRI given for the H → L electronic transition are in a general good accordance with the enhanced bands observed in the resonance Raman spectrum recorded at the 488 nm excitation wavelength and corresponding to maximum absorption of the Q band. As a matter of comparison, the predicted RRI obtained from an equal participation of the four monoelectronic transitions (25% each) are also given in the table.

The general agreement between the predicted and experimental RRI gives some confidence to the force field obtained from the DFT method as an incorrect potential energy distribution would lead to erroneous predicted resonance Raman bands. Moreover, the predicted resonance Raman intensities corresponding to the unscaled DFT-derived force field (all scaling factors being equal to 1) are equally reported in this table. No marked changes between predicted RRI obtained with or without a set of scaling factors could be detected. The meaning of this fact stands in the high values of the scaling factors, and consequently, the potential energy distribution gives comparable participations of the internal coordinates to the normal modes.

The predicted relative resonance Raman intensities for the normal modes with A_g symmetry appearing at 1607, 1490, 1349, and 1174 cm^{-1} correlate well with the experimental enhancements. The experimental RRI were estimated from the peak heights observed in the spectrum recorded at 488 nm[2] with the most intense band being normalized to 10. The corresponding wavenumbers were predicted at 1601, 1508, 1351, and 1178 cm^{-1} and involve principally C_mC_α, $C_\beta C_\beta$, and $C_\beta C_\alpha$ stretching and bending δCNC in-plane motions as it can be observed from the potential energy distribution.

The very intense RRI (7.4) observed at 1314 cm^{-1} at the 488 nm excitation wavelength[2] corresponds here to a B_{1g} mode calculated at 1322 cm^{-1}. No resonance intensity could be calculated for this mode as the method proposed here to calculate the RRI applies only to totally symmetric modes. This is an indirect way to confirm the non-totally symmetric nature of this normal mode.

In the Q-band region, the A_g and B_{3g} modes give rise to resonance Raman enhancements while, in the Soret band near 380−400 nm, only the Ag modes should undergo such enhancements.[5]

The small RRI (1.0) observed at 1136 cm^{-1} corresponds to the predicted B_{1g} mode at 1133 cm^{-1}. For the same reasons as previously, no RRI could be predicted for this mode.

Two normal modes with A_g symmetry are predicted at 1064 and 1055 cm^{-1} with calculated RRI of 8.4 and 0.7 for the H → L transition and RRI of 5.47 and 2.50 in the case of an equal

TABLE 10: Calculated Relative Resonance Raman Intensities (RRI) As Obtained from the Estimation of the Changes in Bond Orders along the Electronic Transition Corresponding to the Q Band Observed at 488 nm for the Free Base Porphine with D_{2h} Symmetry[a]

exp (cm^{-1})	RRI^{exp}	calc (cm^{-1})	sym	RRI^{calc}(H → L)	calc[b]	RRI^{calc}(H → L)[b]	RRI^{calc}(all MO)
1666	1.2						
1643	1.2						
1607	10.0	1601	A_g	10.0	1656	10.0	10.0
1580	1.6	1592	B_{1g}				
1558	0.8	1548	A_g	0.7	1603	0.7	0.98
1541	0.8						
1490	5.4	1508	A_g	5.4	1552	5.1	4.9
1446	1.0						
1425	1.0	1424	A_g	4.2	1476	5.3	4.64
1402	0.0	1399	A_g	4.0	1442	3.4	4.80
1384	0.0	1381	B_{1g}	0.0			
1349	2.1	1351	A_g	3.0	1386	3.5	2.5
1314	7.4	1322	B_{1g}				
1191[sh]	0.9	1184	B_{1g}	0.0			
1174	2.9	1178	A_g	2.5	1208	2.7	1.60
1136	1.0	1133	B_{1g}	0.0			
1086	4.6						
1062	3.7	1064	A_g	8.4	1092	8.4	5.47
1049	1.6	1055	A_g	0.7	1083	0.5	2.5
985	3.3	985	A_g	0.8	1014	0.6	0.82
950	1.6	948	A_g	0.	976	0	0.75
736	4.9	723	A_g	2.0	737	2.3	1.44
721	2.0	719	A_g	1.0	734	0.7	0.82
558	3.0						

[a] sh: shoulder. RRI are calculated for an equal participation of the four monoelectronic transitions (all MO). [b] Values given for a scaling factor of 1.

participation of the four orbitals. The corresponding observed values are 3.7 and 1.6. These last calculated RRI are in better agreement with the experimental ones. The associated potential energy distribution implies $C_\alpha C_\beta H$ and $C_\beta C_\beta H$ in-plane bending vibrations and the frequency shifts observed in the experimental spectrum for the d_8 isotopomer (944 and 959 cm^{-1}) are correctly predicted at 937 and 958 cm^{-1} leading to some confidence with the normal mode description. From this it follows that a particular linear combination of monoelectronic transitions should have better to be used than a particular one. Nakatsuji et al.,[24] using SAC-CI calculations, pointed out the fact that a lone pair orbital ($4b_{1u}$) could also pertub the four-orbital model; this could explain the differences between the values of the calculated and experimental RRI.

As a matter of discrepancy, a normal mode with A_g symmetry observed at 1402 cm^{-1} in the normal Raman spectrum[5] is calculated here at 1399 cm^{-1} with a surprising strong RRI (4.0). No counterpart could be observed in the resonance Raman spectra recorded for the 488 nm excitation (Q band). As was pointed out by Kozlowski et al.,[5] no corresponding resonance enhancement could be observed in the Soret region for FBP. We obtained the same feature as described by these authors. They could observe a Raman band at 1400 cm^{-1} (calculated at 1402 cm^{-1}) and found a corresponding phosphorescence line at 1405 cm^{-1}. They calculated a much larger intensity for this particular band than for the observed one and, finally, assigned this band to an A_{1g} mode and the neighboring one observed at 1384 cm^{-1} to a mode with B_{1g} symmetry. We can confirm this assignment for the 1402 cm^{-1} Raman band, but the reason for which no experimental RRI could be observed is not clear and may be due to interferences between the FC and HT mechanisms.[5]

The A_g mode observed at 985 cm^{-1} is calculated at the same wavelength with a lower resonance intensity (0.80) than observed (3.3), while no RRI intensity could be calculated for the A_g mode observed at 950 cm^{-1} (predicted at 948 cm^{-1}) if one takes only the H → L transition into account. However, a small RRI could be predicted (0.75, observed 1.6) if the four monoelectronic transitions are taken into account. These two modes are mainly $\nu C_\alpha C_\beta$ and νCN in character with a larger participation of the δCNH and $\delta C_\alpha C_\beta H$ in-plane motions for the highest frequency. The corresponding wavenumbers observed in the d_8 isotopomer at 794 and 776 cm^{-1} are correctly reproduced for these two modes.

The doublet at 736 and 721 cm^{-1} observed in the resonance Raman[2] spectrum at 488 nm is well reproduced in the present work by the two predicted bands at 723 and 719 cm^{-1}. The corresponding predicted RRI (2.0 and 1.0) are somewhat less intense than in the experimental spectrum (4.9 and 2.0), but their mutual relative intensities are in agreement with the experiment. These two bands involve $C_\alpha C_m$ and pyrrole ring in-plane bending modes. No dependence on the hydrogen substituents was predicted, this being in agreement with the observation of only a very weak shift in the isotopomer.

Conclusion

The accordance between the present assignments for the d_0, d_2, d_4, d_8, and d_{12} isotopomers of the free base porphyrin and previous normal-mode analysis using a quantum scaled force field leads to the conclusion of two important points: (i) The use of symmetry or internal coordinates to treat the redundancy problem does not change in a large way the assigments of the normal modes. (ii) The determination of the resonance Raman intensities appears to be a good way to identify the totally symmetric modes for a complex molecule such as the free base porphyrin. The normal Raman band with A_g symmetry observed at 1402 cm^{-1} would have to be studied in more detail to explain its lack of experimental resonance Raman intensity and its too strong calculated Raman intensity.

The determination of the resonance Raman intensities appears as a complementary tool to the vibrational analysis and determination of Raman or infrared intensities. The knowledge of the ground electronic state is enough to explain the principal features observed along the resonance Raman enhancements. When dealing with quantum studies, this method is easy to use.

In the case of metalloporphyrins, vibrational wavenumbers will be perturbated for a certain number of bands that are involved in the interactions with the metal. The resonance Raman enhancements would also depend on such interactions, and then the determination of these changes could be related to the electronic transition of the porphine base when linked to the metal ligand.

We have shown that the determination of the RRI is a very restrictive method when dealing with various force fields and that only a force field was possible to retrieve the RRI.

The next application of the determination of the resonance Raman intensities will be done for the metalloporphyrins, and the normal modes having totally symmetric motions will be particularly studied.

References and Notes

(1) Solovyov, K. Y.; Gladkov, L. L.; Gradyushko, A. T.; Ksenofontova, N. M.; Shulga, A. M.; Starukhin, A. S. *J. Mol. Struct.* **1978**, *45*, 267.

(2) Verma, A. L.; Bernstein, H. *J. Biochem. Biophys. Res. Commun.* **1974**, *57*-1, 255.

(3) Radziszewski, J. G.; Nepras, M.; Balaji, V.; Waluk, J.; Vogel, E.; Michl, J. *J. Phys. Chem.* **1995**, *99*, 14254.

(4) Kozlowski, P. M.; Jarzęçki, A. A.; Pulay, P. *J. Phys. Chem.* **1996**, *100*, 7007.

(5) Kozlowski, P. M.; Jarzęçki, A. A.; Pulay, P. *J. Phys. Chem.* **1996**, *100*, 13985.

(6) P. Lagant, P.; Gallouj, H.; Vergoten, G. *J. Mol. Struct.* **1995**, *53*, 372.

(7) Gallouj, H.; Lagant, P.; Vergoten, G. *J. Raman Spectrosc.* **1997**, *28*, 909.

(8) Gallouj, H.; Lagant, P.; Vergoten, G. *J. Raman Spectrosc.* **1998**, *29*, 343.

(9) Lagant, P.; Derreumaux, P.; Vergoten, G.; Peticolas, W. L. *J. Comput. Chem.* **1991**, *12*, 731.

(10) Lagant, P.; Elass, A.; Dauchez, M.; Vergoten, G. *Spectrochim. Acta, Part A* **1992**, *48*, 1323

(11) Lagant, P.; Vergoten, G.; Efremov, R.; Peticolas, W. L. *Spectrochim. Acta, Part A* **1994**, *50*, 961.

(12) Lagant, P.; Vergoten, G.; Peticolas, W. L. *Biospectroscopy* **1998**, *4*, 379.

(13) Jaguar v3.0, Schrödinger, Inc., Portland, OR, 1997.

(14) Spartan v5.0, Wavefunction, Inc., Irvine, CA, 1997.

(15) Allouche, A.; Pourcin, J. *Spectrochim. Acta, Part A* **1970**, *49*, 2086.

(16) Li, X. Y.; Zgierski, M. Z. *J. Phys. Chem.* **1991**, *95*, 4268.

(17) Chen, B. M. L.; Tulinski, A. *J. Am. Chem. Soc.* **1972**, *94*, 4144.

(18) Matsuzawa, M.; Ata, M.; Dixon, D. A. *J. Phys. Chem.* **1995**, *99*, 7698.

(19) Ghosh, A.; Almlöf, J. *Chem. Phys. Lett.* **1993**, *213*, 519.

(20) Almöf, J.; Fischer, T. H.; Gassman, P. G.; Ghosh, A.; Häser, M. *J. Phys. Chem.* **1993**, *97*, 10964.

(21) Wilson, E. B.; Decius, J. C.; Cross, P. C. *Molecular Vibrations*; McGraw-Hill: New York, 1955.

(22) Blazej, D. C.; Peticolas, W. L. *Proc. Natl. Acad. Sci. U.S.A.* **1977**, *74*, 2639.

(23) Peticolas, W. L.; Strommen, D. P.; Lakshminarayanan, V. *J. Chem. Phys.* **1980**, *73*, 4185.

(24) Nakatsuji, H.; Hasegawa, J. Y.; Hada, M. *J. Chem. Phys.* **1996**, *104*, 2321.

(25) Gouterman, M. *The Porphyrins*; Dolphin, Ed.; Academic: New York, 1977; Vol. 3.

(26) Lamoen, D.; Parrinello, M. *Chem. Phys. Lett.* **1996**, *248*, 309.

(27) Merchan, M.; Orti, E.; Roos, B. O. *Chem. Phys. Lett.* **1994**, *221*, 136.